ESAIM: M2AN 58 (2024) 1137–1151
https://doi.org/10.1051/m2an/2024036

ESAIM: Mathematical Modelling and Numerical Analysis
www.esaim-m2an.org

OPTIMAL DESIGN OF ELASTIC PLATES

Ivana Crnjac[1], Jelena Jankov Pavlović[1] and Petar Kunštek[2,*]

Abstract. This paper is concerned with optimal design problems in the setting of the Kirchhoff–Love model for pure bending of a thin solid symmetric plate under a transverse load. For two isotropic elastic materials with a prescribed amount, the goal is to find their rearrangement within the domain that forms a least compliant structure. The homogenization method is used as a relaxation tool to overcome the lack of a classical solution of optimal design problem. Neccessary conditions of optimality were derived and an optimality criteria method for the single state compliance minimization problems is developed and tested on several examples.

Mathematics Subject Classification. 49M05, 49J20, 74Q05, 74K20, 35J30.

Received April 26, 2023. Accepted May 13, 2024.

1. Introduction

Structural optimization is the process whose main goal is to minimize the total cost of construction, and it is a fundamental concept of any optimal design process in civil engineering. There is a huge number of applications of such problems, *e.g.* in aeronautics, design of flexible structures, location of pollutants, optical fibers, etc. We will explore optimal design problems in the context of the Kirchhoff–Love plate, so we start by setting the problem more presicely. We consider a homogeneous Dirichlet boundary value problem for a general fourth-order partial differential equation, *i.e.* we assume that the plate is clamped at the boundary and, according to the Kirchhoff–Love model, the governing boundary-value problem is

$$\begin{cases} \mathsf{div}\,\mathsf{div}\,(\mathbf{M}\nabla\nabla u) = f \text{ in } \Omega \\ u \in \mathrm{H}^2_0(\Omega). \end{cases} \tag{1.1}$$

Here, $\Omega \subseteq \mathbf{R}^2$ is a bounded region representing the midplane of the plate with respect to which it is symmetric. The vertical displacement u of the plate is uniquely determined by the transverse load $f \in \mathrm{H}^{-2}(\Omega)$. The elastic properties of the plate are described by a tensor valued function $\mathbf{M}$, also called the stiffness tensor. We assume that $\mathbf{M}$ belongs to the space $\mathrm{L}^\infty(\Omega; \mathcal{L}(\mathrm{Sym}, \mathrm{Sym}))$, where $\mathcal{L}(\mathrm{Sym}, \mathrm{Sym})$ is the space of all linear operators that act on the space of symmetric matrices Sym and take values in Sym. Furthermore, for some $0 < \alpha < \beta$, we

Keywords and phrases. Kirchhoff–Love model of elastic plate, optimal design, optimality criteria method, Hashin–Shtrikman bounds.

[1] School of Applied Mathematics and Informatics, University of Osijek, Osijek, Croatia.
[2] Department of Mathematics, Faculty of Science University of Zagreb, Zagreb, Croatia.
*Corresponding author: petar@math.hr

assume that function $\mathbf{M}$ satisfies (a.e. $\mathbf{x} \in \Omega$)

$$\mathbf{M}(\mathbf{x})\mathbf{S} : \mathbf{S} \geq \alpha \mathbf{S} : \mathbf{S} \ \& \ \mathbf{M}(\mathbf{x})^{-1}\mathbf{S} : \mathbf{S} \geq \frac{1}{\beta}\mathbf{S} : \mathbf{S}, \quad \mathbf{S} \in \mathrm{Sym},$$

where ":" denotes the standard inner product on Sym.

In the sequel, we shall present the general theory in arbitrary space dimension d, unless it is explicitly stated otherwise. We shall restrict ourselves on the stiffness tensor made up of two materials $\mathbf{A}$ and $\mathbf{B}$, which can be represented by formula

$$\mathbf{M}(\mathbf{x}) = \chi(\mathbf{x})\mathbf{A} + (1 - \chi(\mathbf{x}))\mathbf{B}, \quad \mathbf{x} \in \Omega,$$

for $\chi \in \mathrm{L}^\infty(\Omega; \{0,1\})$ being the characteristic function of a part of the domain occupied by material $\mathbf{A}$. Moreover, we assume well-ordered and isotropic materials within Ω,

$$\mathbf{A} = 2\mu_{\mathbf{A}}\mathbf{I}_4 + \left(\kappa_{\mathbf{A}} - \frac{2\mu_{\mathbf{A}}}{d}\right)\mathbf{I}_2 \otimes \mathbf{I}_2$$
$$\mathbf{B} = 2\mu_{\mathbf{B}}\mathbf{I}_4 + \left(\kappa_{\mathbf{B}} - \frac{2\mu_{\mathbf{B}}}{d}\right)\mathbf{I}_2 \otimes \mathbf{I}_2,$$

where $0 < \kappa_{\mathbf{A}} \leq \kappa_{\mathbf{B}}$ are the bulk moduli, $0 < \mu_{\mathbf{A}} \leq \mu_{\mathbf{B}}$ are the shear moduli, $\mathbf{I}_4 \in \mathcal{L}(\mathrm{Sym}, \mathrm{Sym})$ is the identity operator defined by $\mathbf{I}_4\boldsymbol{\eta} = \boldsymbol{\eta}$, $\boldsymbol{\eta} \in \mathrm{Sym}$, while $\mathbf{I}_2$ denotes identity matrix in $M_d(\mathbf{R})$. If $q \in (0, |\Omega|)$ is the prescribed volume of material $\mathbf{A}$ in the domain, then the problem of optimal design reads

$$\begin{cases} J(\chi) = \int_\Omega [\chi(\mathbf{x})g_1(\mathbf{x}, \mathsf{u}(\mathbf{x})) + (1 - \chi(\mathbf{x}))g_2(\mathbf{x}, \mathsf{u}(\mathbf{x}))] \,\mathrm{d}\mathbf{x} \longrightarrow \min, \\ \chi \in \mathrm{L}^\infty(\Omega; \{0,1\}), \ \int_\Omega \chi \,\mathrm{d}\mathbf{x} = q. \end{cases} \tag{1.2}$$

Function u is the solution to the boundary value problem (1.1), and g_1, g_2 are Carathéodory functions which satisfy the growth condition

$$|g_k(\mathbf{x}, \mathsf{u})| \leq a|\mathsf{u}|^s + b(\mathbf{x}), \quad k \in \{1,2\},$$

for some $a > 0$, $b \in \mathrm{L}^1(\Omega)$ and $1 \leq s < \frac{2d}{d-2}$ (in dimensions $d = 1$ or $d = 2$, the exponent s has to be understood in the sense that $1 \leq s < \infty$). The classical solution for the above minimization problem usually does not exist and one should consider properly relaxing the original problem. Due to its wide application, there are several different approaches to the mathematical theory of optimal design. One of the most successful approaches is homogenization method, introduced by Murat and Tartar [37] for problems of optimal design in conductivity, and afterwards adapted to the elasticity setting [22,28,40], particularly in the context of elastic plate [7,8]. The homogenization method allows one to find a global minimizer in most instances, at the price of introducing generalized designs, also called composite materials [1,20,33]. A generalized design is a couple $(\theta, \mathbf{M})$, with θ representing the local fraction of the first material in a mixture, while $\mathbf{M}$ is the homogenized elasticity tensor containing information on how the materials are mixed.

One of the interesting representatives of a generalized design are laminated materials, which are widely distributed in various industries, including construction, electronics, aerospace, etc. In these composites, the original phases are stacked in layers orthogonal to some given direction. More precisely, for two phases $\mathbf{A}$ and $\mathbf{B}$, a unit vector $\mathbf{e} \in \mathbf{R}^d$, and some $\theta \in [0,1]$, the homogenized tensor $\mathbf{M}$ obtained by a simple lamination of phases $\mathbf{A}$ and $\mathbf{B}$ in proportions θ and $(1 - \theta)$, and in the direction $\mathbf{e}$, is given by

$$\mathbf{M} = \theta\mathbf{A} + (1-\theta)\mathbf{B} - \frac{\theta(1-\theta)(\mathbf{A} - \mathbf{B})(\mathbf{e} \otimes \mathbf{e}) \otimes (\mathbf{A} - \mathbf{B})^T(\mathbf{e} \otimes \mathbf{e})}{(1-\theta)\mathbf{A}(\mathbf{e} \otimes \mathbf{e}) : (\mathbf{e} \otimes \mathbf{e}) + \theta\mathbf{B}(\mathbf{e} \otimes \mathbf{e}) : (\mathbf{e} \otimes \mathbf{e})} \tag{1.3}$$

which is referred to as a simple laminate [14]. This lamination formula can be equivalently expressed in terms of inverse tensors $\mathbf{A}^{-1}$ and $\mathbf{B}^{-1}$ as

$$\theta(\mathbf{M}^{-1} - \mathbf{B}^{-1})^{-1} = (\mathbf{A}^{-1} - \mathbf{B}^{-1})^{-1} + (1-\theta)\left[\mathbf{B} - \mathbf{B}\frac{(\mathbf{e} \otimes \mathbf{e}) \otimes (\mathbf{e} \otimes \mathbf{e})}{\mathbf{B}(\mathbf{e} \otimes \mathbf{e}) : (\mathbf{e} \otimes \mathbf{e})}\mathbf{B}\right]. \tag{1.4}$$

It is of interest to consider a particular subset of laminated materials, obtained by an iterative process of lamination, where the previous laminate is laminated again with a single pure phase (always the same one, *e.g.* B). In this way, if we repeat an iterative process of lamination p times, in directions e_i, $i = 1, \dots, p$, we obtain a composite material A_p^* called a *rank-p sequential laminate* with matrix B and core A, which is determined by the formula

$$\theta\big(\mathsf{A}_p^* - \mathsf{B}\big)^{-1} = (\mathsf{A} - \mathsf{B})^{-1} + (1-\theta)\sum_{i=1}^{p} m_i \frac{(\mathbf{e}_i \otimes \mathbf{e}_i) \otimes (\mathbf{e}_i \otimes \mathbf{e}_i)}{\mathsf{B}(\mathbf{e}_i \otimes \mathbf{e}_i) : (\mathbf{e}_i \otimes \mathbf{e}_i)}, \tag{1.5}$$

where $m_i \geq 0$, $i = 1, \dots, p$ are lamination parameters that satisfy $\sum_{i=1}^{p} m_i = 1$. The overall volume fraction of material A in this rank-p sequential laminate is $\theta = \prod_{i=1}^{p} \theta_i$, where θ_i denotes the proportion of phase A in i-th lamination. The proportions of the first phase in each lamination can be obtained from the lamination parameters and the overall volume fraction θ by solving the system

$$(1-\theta)m_i = (1-\theta_i)\prod_{j=1}^{i-1}\theta_j, \quad i = 1, \dots, p.$$

As for simple laminates, the sequential laminate (1.5) can be equivalently expressed by

$$\theta\Big(\mathsf{A}_p^{*-1} - \mathsf{B}^{-1}\Big)^{-1} = \big(\mathsf{A}^{-1} - \mathsf{B}^{-1}\big)^{-1} + (1-\theta)\left[\mathsf{B} - \sum_{i=1}^{p} m_i \mathsf{B}\frac{(\mathbf{e}_i \otimes \mathbf{e}_i) \otimes (\mathbf{e}_i \otimes \mathbf{e}_i)}{\mathsf{B}(\mathbf{e}_i \otimes \mathbf{e}_i) : (\mathbf{e}_i \otimes \mathbf{e}_i)}\mathsf{B}\right]. \tag{1.6}$$

One could interchange the roles of A and B and obtain a symmetric class of sequential laminates, *i.e.*, a rank-p sequential laminate with matrix A and core B.

In addition to laminated materials, for given phases A and B and some $\theta \in [0,1]$, it is interesting to find the set G_θ of all possible homogenized tensors M that can be obtained by mixing these materials in proportions θ and $(1-\theta)$. This is a well-known G-closure problem, and the explicit characterization of the G-closure set has been done in the conductivity settings for mixtures of two isotropic conductors [30, 41], while in the elasticity settings, it is still an open problem (for partial results, we refer to [34] and references therein), even for elastic plates [25, 32].

Using the relaxation by the homogenization method and introducing the Lagrange multiplier l to handle the volume constraint of the first phase, the proper relaxation of optimal design problem (1.2) reads

$$\begin{cases} J(\theta, \mathbf{M}) := \int_\Omega [\theta(\mathbf{x})g_1(\mathbf{x}, \mathsf{u}(\mathbf{x})) + (1-\theta)(\mathbf{x}))g_2(\mathbf{x}, \mathsf{u}(\mathbf{x}))]\,\mathrm{d}\mathbf{x} + l\int_\Omega \theta(\mathbf{x})\,\mathrm{d}\mathbf{x} \longrightarrow \min, \\ (\theta, \mathbf{M}) \in \mathrm{L}^\infty(\Omega; [0,1] \times \mathcal{L}(\mathrm{Sym}, \mathrm{Sym}));\ \mathbf{M}(\mathbf{x}) \in G_{\theta(\mathbf{x})} \text{ a.e. on } \Omega. \end{cases} \tag{1.7}$$

Lack of information about G-closure can partially be compensated by the knowledge of Hashin–Shtrikman bounds [26], which are bounds on the effective energy of a composite material. They are well known in the context of elasticity [4, 17, 18], particularly for plates, as documented in [14, 25]. The bounds can be stated in terms of strain $\mathsf{A}\boldsymbol{\xi} : \boldsymbol{\xi}$ or in terms of stress $\mathsf{A}^{-1}\boldsymbol{\sigma} : \boldsymbol{\sigma}$. We provide them in terms of stress, *i.e.*, we give the lower and the upper Hashin–Shtrikman bound on the complementary (or dual) energy [13].

Theorem 1.1. *For fixed* $\theta \in [0,1]$, *every homogenized tensor* $\mathsf{A}^* \in G_\theta$ *satisfies for all* $\boldsymbol{\sigma} \in \mathrm{Sym}$

$$\mathsf{A}^{*-1}\boldsymbol{\sigma} : \boldsymbol{\sigma} \geq \mathsf{B}^{-1}\boldsymbol{\sigma} : \boldsymbol{\sigma} + \theta \max_{\boldsymbol{\eta} \in \mathrm{Sym}}\Big[2\boldsymbol{\sigma} : \boldsymbol{\eta} - \big(\mathsf{A}^{-1} - \mathsf{B}^{-1}\big)^{-1}\boldsymbol{\eta} : \boldsymbol{\eta} - (1-\theta)g^c(\boldsymbol{\eta})\Big], \tag{1.8}$$

where

$$g^c(\boldsymbol{\eta}) := \mathsf{B}\boldsymbol{\eta} : \boldsymbol{\eta} - h_{\mathsf{B}}(\boldsymbol{\eta}),$$

while $h_{\mathbf{B}}(\boldsymbol{\eta})$ *is defined with*

$$h_{\mathbf{B}}(\boldsymbol{\eta}) := \min_{\mathbf{e}\in S^{d-1}} \frac{|(\mathbf{e}\otimes\mathbf{e}) : \mathbf{B}\boldsymbol{\eta}|^2}{\mathbf{B}(\mathbf{e}\otimes\mathbf{e}) : (\mathbf{e}\otimes\mathbf{e})}.$$

Moreover for all $\boldsymbol{\sigma} \in \mathrm{Sym}$,

$$\mathbf{A}^{*-1}\boldsymbol{\sigma} : \boldsymbol{\sigma} \leq \mathbf{A}^{-1}\boldsymbol{\sigma} : \boldsymbol{\sigma} + (1-\theta) \min_{\boldsymbol{\eta}\in\mathrm{Sym}} \left[2\boldsymbol{\sigma} : \boldsymbol{\eta} + \left(\mathbf{A}^{-1} - \mathbf{B}^{-1}\right)^{-1}\boldsymbol{\eta} : \boldsymbol{\eta} - \theta h^c(\boldsymbol{\eta})\right], \tag{1.9}$$

where

$$h^c(\boldsymbol{\eta}) := \mathbf{A}\boldsymbol{\eta} : \boldsymbol{\eta} - g_{\mathbf{A}}(\boldsymbol{\eta}),$$

while $g_{\mathbf{A}}(\boldsymbol{\eta})$ *is defined with*

$$g_{\mathbf{A}}(\boldsymbol{\eta}) := \max_{\mathbf{e}\in S^{d-1}} \frac{|(\mathbf{e}\otimes\mathbf{e}) : \mathbf{A}\boldsymbol{\eta}|^2}{\mathbf{A}(\mathbf{e}\otimes\mathbf{e}) : (\mathbf{e}\otimes\mathbf{e})}.$$

Additionally, equations (1.8) *and* (1.9) *are optimal: the optimality of the bound* (1.8) *is achieved by a rank-p sequential laminate* (1.6), *while optimality of the bound* (1.9) *is achieved by a rank-p sequential laminate with core* $\mathbf{B}$ *and matrix* $\mathbf{A}$, *where* $p = 1 + (d+3)(d+2)(d+1)d/24$.

It is unlikely to find an analytical solution to problem (1.7) (for some simple cases see [11, 15, 19, 36, 42]), so various numerical methods are used for finding approximate solutions. There are a number of results regarding numerical solutions to problems of optimal design in elasticity setting [5,6,12,17,23,29,31,32]. One of the popular numerical methods is optimality criteria method, which is based on the neccessary conditions of optimality for the relaxed problem [9,39]. In the case of compliance minimization, the lower Hashin–Shtrikman bound naturally appears in the neccessary conditions of optimality, so there is a need for its explicit form in order to develop an optimality criteria method. Novel results on homogenization in the context of elastic plate equation [14,16], particularly one regarding Hashin–Shtrikman bounds [13] enables us to derive another variant of the optimality criteria method.

The remainder of the paper is structured as follows. Section 2 derives the necessary optimality conditions for a specific objective functional, namely the compliance, which aims at maximizing the rigidity of the body under load. This leads to the most rigid design possible. Section 3 presents numerical examples of optimal design problems for elastic plates.

2. Compliance minimization

Hashin–Shtrikman bounds enables us to find a solution of the relaxed problem (1.7) in some special cases, like self-adjoint problems or eigenfrequency optimization. Therefore, in the following, for u being the soluton of the elastic plate equation (1.1), we set $g_1 = g_2 = fu$. The objective functional in (1.7) then reduces to

$$J(\theta, \mathbf{M}) = \int_\Omega f(\mathbf{x})u(\mathbf{x})\,\mathrm{d}\mathbf{x} + l\int_\Omega \theta(\mathbf{x})\,\mathrm{d}\mathbf{x}. \tag{2.1}$$

The quantity $\int_\Omega fu\,\mathrm{d}\mathbf{x}$ is known as the compliance, which represents the work done by the load. Minimizing (2.1) allows us to find the most rigid structure made of elastic materials $\mathbf{A}$ and $\mathbf{B}$ in the presence of the Lagrange multiplier term.

Remark 2.1. The compliance function can itself be written as a minimization problem. To see this, first recall that a weak solution of the elastic plate equation (1.1) by the principle of complementary energy can equivalently be characterized as a unique minimizer of the quadratic functional

$$\frac{1}{2}\int_\Omega \mathbf{M}\nabla\nabla v : \nabla\nabla v\,\mathrm{d}\mathbf{x} - \int_\Omega fv\,\mathrm{d}\mathbf{x}, \quad v \in \mathrm{H}^2_0(\Omega).$$

For $\boldsymbol{\xi} = \nabla\nabla v - \mathbf{M}^{-1}\boldsymbol{\tau}$, $v \in \mathrm{H}^2_0(\Omega)$, $\boldsymbol{\tau} \in \mathrm{L}^2(\Omega; \mathrm{Sym})$, coercivity of $\mathbf{M}$ and monotonicity of an integral implies

$$-\int_\Omega \mathbf{M}^{-1}\boldsymbol{\tau} : \boldsymbol{\tau}\,\mathrm{d}\mathbf{x} \leq \int_\Omega (\mathbf{M}\nabla\nabla v : \nabla\nabla v - 2\boldsymbol{\tau} : \nabla\nabla v)\,\mathrm{d}\mathbf{x}, \quad \text{a.e. } \mathbf{x} \in \Omega.$$

Equality in the above inequality is achieved if and only if $\nabla\nabla v - \mathbf{M}^{-1}\boldsymbol{\tau} = \mathbf{0}$ (since $\mathbf{M}$ is positive semidefinite), which happens if and only if $\boldsymbol{\tau} = \mathbf{M}\nabla\nabla v$. By maximizing over the set of all $\boldsymbol{\tau} \in \mathrm{L}^2(\Omega; \mathrm{Sym})$ such that $\operatorname{div}\operatorname{div}\boldsymbol{\tau} = f$ in Ω, it follows

$$-\min_{\substack{\boldsymbol{\tau}\in \mathrm{L}^2(\Omega;\mathrm{Sym})\\ \operatorname{div}\operatorname{div}\boldsymbol{\tau}=f \text{ in } \Omega}} \int_\Omega \mathbf{M}^{-1}\boldsymbol{\tau} : \boldsymbol{\tau}\,\mathrm{d}\mathbf{x} = \int_\Omega (\mathbf{M}\nabla\nabla v : \nabla\nabla v - 2fv)\,\mathrm{d}\mathbf{x}, \quad v \in \mathrm{H}^2_0(\Omega).$$

Therefore, for the solution u of (1.1) we have

$$-\int_\Omega fu\,\mathrm{d}\mathbf{x} = \int_\Omega (\mathbf{M}\nabla\nabla u : \nabla\nabla u - 2fu)\,\mathrm{d}\mathbf{x} = -\min_{\substack{\boldsymbol{\tau}\in \mathrm{L}^2(\Omega;\mathrm{Sym})\\ \operatorname{div}\operatorname{div}\boldsymbol{\tau}=f \text{ in } \Omega}} \int_\Omega \mathbf{M}^{-1}\boldsymbol{\tau} : \boldsymbol{\tau}\,\mathrm{d}\mathbf{x}.$$

Furthermore, the functional (2.1) becomes

$$J(\theta, \mathbf{M}) = \min_{\substack{\boldsymbol{\tau}\in \mathrm{L}^2(\Omega;\mathrm{Sym})\\ \operatorname{div}\operatorname{div}\boldsymbol{\tau}=f \text{ in } \Omega}} \int_\Omega \mathbf{M}^{-1}\boldsymbol{\tau} : \boldsymbol{\tau}\,\mathrm{d}\mathbf{x} + l\int_\Omega \theta\,\mathrm{d}\mathbf{x}, \tag{2.2}$$

where the minimum on the right-hand side is achieved by $\boldsymbol{\tau} = \mathbf{M}\nabla\nabla u$.

Due to the above remark, the relaxed problem (1.7) can be considered as a double minimization in $(\theta, \mathbf{M})$ and in $\boldsymbol{\tau}$. The sets by which the minimization is performed are independent, thus we obtain

$$\min_{(\theta,\mathbf{M})\in\mathcal{A}} J(\theta, \mathbf{M}) = \min_{\substack{\boldsymbol{\tau}\in \mathrm{L}^2(\Omega;\mathrm{Sym})\\ \operatorname{div}\operatorname{div}\boldsymbol{\tau}=f \text{ in } \Omega}} \min_{(\theta,\mathbf{M})\in\mathcal{A}} \int_\Omega \left(\mathbf{M}^{-1}\boldsymbol{\tau} : \boldsymbol{\tau} + l\theta\right)\mathrm{d}\mathbf{x}. \tag{2.3}$$

This approach is adequate for deriving the necessary conditions of optimality, stated in the following theorem.

Theorem 2.1. *If $(\theta^*, \mathbf{M}^*)$ is a minimizer of the objective function (2.1), and if $\boldsymbol{\sigma}^*$ is the unique corresponding minimizer in (2.2), then $\boldsymbol{\sigma}^* = \mathbf{M}^*\nabla\nabla u^*$, where u^* is the state function for $(\theta^*, \mathbf{M}^*)$. Furthermore, $\mathbf{M}^*$ satisfies, almost everywhere in Ω,*

$$\mathbf{M}^{*-1}\boldsymbol{\sigma}^* : \boldsymbol{\sigma}^* = h(\theta^*, \boldsymbol{\sigma}^*) := \min_{\mathbf{M}\in G_\theta} \mathbf{M}^{-1}\boldsymbol{\sigma} : \boldsymbol{\sigma}, \tag{2.4}$$

where $h(\theta^*, \boldsymbol{\sigma}^*)$ is the lower Hashin–Shtrikman bound on the complementary energy defined by (1.8), while θ^* is the unique minimizer of the convex minimization problem

$$\min_{0\leq\theta\leq 1} (h(\theta, \boldsymbol{\sigma}^*) + l\theta), \quad \text{a.e. on } \Omega. \tag{2.5}$$

The proof of this theorem follows the same approach as in the case of linearized elasticity ([3], Thm. 4.1.9), and will be omitted. However, it's worth noting that in the case of compliance minimization, an optimal design saturates the lower Hashin–Shtrikman bound on the complementary energy. This implies that the optimal design can be found among laminated materials, rather than any arbitrary composite material. Therefore, instead of minimizing compliance on the set of all composite materials, it's sufficient to perform the minimization on its subset of sequential laminates.

Theorem 2.2. *For the objective function* (2.1) *we have*

$$\min_{(\theta,\mathbf{M})\in\mathcal{A}} J(\theta,\mathbf{M}) = \min_{(\theta,\mathbf{M})\in\mathcal{L}^+} J(\theta,\mathbf{M}),$$

where $\mathcal{L}^+$ is the set of sequentially laminated designs defined as

$$\mathcal{L}^+ := \Big\{(\theta,\mathbf{M}) \in \mathrm{L}^\infty(\Omega;[0,1]\times\mathcal{L}(\mathrm{Sym},\mathrm{Sym})) : \mathbf{M}(\mathbf{x}) \in L^+_{\theta(\mathbf{x})}, \quad \text{a.e. in } \Omega\Big\},$$

where L^+_θ, for $\theta\in[0,1]$, is the set of all sequential laminates $\mathbf{M}$, with core $\mathbf{A}$ and matrix $\mathbf{B}$, in proportions θ and $(1-\theta)$, respectively. If $(\theta^*,\mathbf{M}^*)$ is a minimizer of J in $\mathcal{A}$, and if $\boldsymbol{\sigma}^*$ is its associated stress tensor which minimizes (2.2)*, then there exists a sequential laminate $\widetilde{\mathbf{M}}$ such that $(\theta^*,\widetilde{\mathbf{M}})$ is a minimizer of J in $\mathcal{L}^+$, $\boldsymbol{\sigma}^*$ is again its associated stress tensor, and ${\mathbf{M}^*}^{-1}\boldsymbol{\sigma}^* = \widetilde{\mathbf{M}}^{-1}\boldsymbol{\sigma}^*$.*

Again, the proof is similar to one in Theorem 4.1.12 of [3] and thus will be omitted.

Remark 2.2. According to the Theorem 1.1, $\widetilde{\mathbf{M}}$ in Theorem 2.2 can be chosen among rank-p sequential laminates with core $\mathbf{A}$ and matrix $\mathbf{B}$, where $p = 1 + (d+3)(d+2)(d+1)d/24$.

From the above, we can conclude that the relaxation by the homogenization method is suitable for the development of numerical methods based on the necessary conditions of optimality. Using Theorems 2.1 and 2.2 an optimality criteria method can be derived. The algorithm is as follows:

Algorithm 2.1. Take some initial θ^0 and $\mathbf{M}^0$. For $k\geq 0$:

(1) Calculate u^k, the solution of

$$\begin{cases} \mathsf{div\,div}\left(\mathbf{M}^k\nabla\nabla u^k\right) = f \\ u^k \in \mathrm{H}^2_0(\Omega), \end{cases}$$

and define $\boldsymbol{\sigma}^k := \mathbf{M}^k\nabla\nabla u^k$.

(2) For $\mathbf{x}\in\Omega$, take $\theta^{k+1}(\mathbf{x})$ as the zero of the function

$$\theta \mapsto \frac{\partial h}{\partial\theta}\big(\theta,\boldsymbol{\sigma}^k(\mathbf{x})\big) + l, \tag{2.6}$$

and if a zero doesn't exist, take 0 (or 1) if the function is positive (or negative) on $[0,1]$.

(3) Let $\mathbf{M}^{k+1}(\mathbf{x})$ be the minimizer in the definition of $h(\theta^{k+1}(\mathbf{x}),\boldsymbol{\sigma}^k(\mathbf{x}))$.

Remark 2.3. Algorithm 2.1 actually coincides with the alternate direction algorithm [6], where the minimization of (2.3) is performed iteratively and separately in $\boldsymbol{\sigma}$ and $(\theta,\mathbf{A})$.

To implement Algorithm 2.1, it is necessary to explicitly calculate the lower Hashin–Shtrikman bound on the complementary energy, as well as the corresponding sequential laminates that saturate the bound. Explicit computation of the function $h(\theta,\boldsymbol{\sigma})$ is given in [4, 17, 18], particularly for plates in two space dimensions, it is given in [13] (for shape optimization see [2, 5, 23, 24]). Beside the explicit bound and microstructure that saturate it, the derivation of the bound over θ is needed for the second step of Algorithm 2.1. We present all afore-mentioned for two-dimensional case in the theorem and remark below [13].

Theorem 2.3. *After denoting by σ_1 and σ_2 the eigenvalues of $\boldsymbol{\sigma}$, and $\delta\kappa := \kappa_\mathbf{B} - \kappa_\mathbf{A}$, $\delta\mu := \mu_\mathbf{B} - \mu_\mathbf{A}$, the explicit formula for the bound* (1.8) *in dimension $d = 2$ is given as follows:*

(i) *If*

$$\mu_\mathbf{B}(1-\theta)\delta\kappa|\sigma_1+\sigma_2| < (\kappa_\mathbf{B}(\mu_\mathbf{B}+\kappa_\mathbf{A}) - \theta\mu_\mathbf{B}\delta\kappa)|\sigma_1-\sigma_2| \ \& \tag{2.7}$$

$$\delta\kappa(\mu_{\mathbf{B}} - \theta\delta\mu)|\sigma_1 + \sigma_2| \geq \delta\mu(\kappa_{\mathbf{B}} - \theta\delta\kappa)|\sigma_1 - \sigma_2|,$$

then

$$h(\theta, \boldsymbol{\sigma}) = \left(\theta_1 \mathbf{A}^{-1} + \theta_2 \mathbf{B}^{-1}\right)\boldsymbol{\sigma} : \boldsymbol{\sigma} - \frac{\theta(1-\theta)\left(\mu_{\mathbf{A}}\mu_{\mathbf{B}}\delta\kappa|\sigma_1 + \sigma_2| + \kappa_{\mathbf{A}}\kappa_{\mathbf{B}}\delta\mu|\sigma_1 - \sigma_2|\right)^2}{4\mu_{\mathbf{A}}\mu_{\mathbf{B}}\kappa_{\mathbf{A}}\kappa_{\mathbf{B}}[\mu_{\mathbf{B}}\kappa_{\mathbf{B}}(\mu_{\mathbf{A}} + \kappa_{\mathbf{A}}) - \theta(\mu_{\mathbf{A}}\mu_{\mathbf{B}}\delta\kappa + \kappa_{\mathbf{A}}\kappa_{\mathbf{B}}\delta\mu)]},$$

while

$$\frac{\partial h(\theta, \boldsymbol{\sigma})}{\partial \theta} = -\frac{\left[(1-2\theta)\mu_{\mathbf{B}}\kappa_{\mathbf{B}}(\mu_{\mathbf{A}} + \kappa_{\mathbf{A}}) + \theta^2(\mu_{\mathbf{A}}\mu_{\mathbf{B}}\delta\kappa + \kappa_{\mathbf{A}}\kappa_{\mathbf{B}}\delta\mu)\right]\left(\mu_{\mathbf{A}}\mu_{\mathbf{B}}\delta\kappa|\sigma_1 + \sigma_2| + \kappa_{\mathbf{A}}\kappa_{\mathbf{B}}\delta\mu|\sigma_1 - \sigma_2|\right)^2}{4\mu_{\mathbf{A}}\mu_{\mathbf{B}}\kappa_{\mathbf{A}}\kappa_{\mathbf{B}}[\mu_{\mathbf{B}}\kappa_{\mathbf{B}}(\mu_{\mathbf{A}} + \kappa_{\mathbf{A}}) - \theta(\mu_{\mathbf{A}}\mu_{\mathbf{B}}\delta\kappa + \kappa_{\mathbf{A}}\kappa_{\mathbf{B}}\delta\mu)]^2}.$$

(ii) *If*

$$\delta\kappa(\mu_{\mathbf{B}} - \theta\delta\mu)|\sigma_1 + \sigma_2| < \delta\mu(\kappa_{\mathbf{B}} - \theta\delta\kappa)|\sigma_1 - \sigma_2|, \tag{2.8}$$

then

$$h(\theta, \boldsymbol{\sigma}) = \mathbf{B}^{-1}\boldsymbol{\sigma} : \boldsymbol{\sigma} + \frac{\theta}{4}\left[\frac{\delta\mu(\sigma_1 - \sigma_2)^2}{\mu_{\mathbf{B}}(\mu_{\mathbf{B}} - \theta\delta\mu)} + \frac{\delta\kappa(\sigma_1 + \sigma_2)^2}{\kappa_{\mathbf{B}}(\kappa_{\mathbf{B}} - \theta\delta\kappa)}\right],$$

and

$$\frac{\partial h(\theta, \boldsymbol{\sigma})}{\partial \theta} = \frac{1}{4}\left[\frac{\delta\mu(\sigma_1 - \sigma_2)^2}{(\mu_{\mathbf{B}} - \theta\delta\mu)^2} + \frac{\delta\kappa(\sigma_1 + \sigma_2)^2}{(\kappa_{\mathbf{B}} - \theta\delta\kappa)^2}\right].$$

(iii) *If*

$$\mu_{\mathbf{B}}(1-\theta)\delta\kappa|\sigma_1 + \sigma_2| \geq (\kappa_{\mathbf{B}}(\mu_{\mathbf{B}} + \kappa_{\mathbf{A}}) - \theta\mu_{\mathbf{B}}\delta\kappa)|\sigma_1 - \sigma_2|, \tag{2.9}$$

then

$$h(\theta, \boldsymbol{\sigma}) = \mathbf{B}^{-1}\boldsymbol{\sigma} : \boldsymbol{\sigma} + \frac{\theta\delta\kappa(\mu_{\mathbf{B}} + \kappa_{\mathbf{B}})(\sigma_1 + \sigma_2)^2}{4\kappa_{\mathbf{B}}[\kappa_{\mathbf{B}}(\mu_{\mathbf{B}} + \kappa_{\mathbf{A}}) - \mu_{\mathbf{B}}\delta\kappa\theta]},$$

and

$$\frac{\partial h(\theta, \boldsymbol{\sigma})}{\partial \theta} = \frac{\kappa_{\mathbf{B}}\delta\kappa(\mu_{\mathbf{B}} + \kappa_{\mathbf{B}})(\mu_{\mathbf{B}} + \kappa_{\mathbf{A}})(\sigma_1 + \sigma_2)^2}{4\kappa_{\mathbf{B}}[\kappa_{\mathbf{B}}(\mu_{\mathbf{B}} + \kappa_{\mathbf{A}}) - \mu_{\mathbf{B}}\delta\kappa\theta]^2}.$$

Cases (i)–(iii) are disjoint, and the union of all $(\sigma_1, \sigma_2) \in \mathbf{R}^2$ *which satisfy one of the conditions* (2.7)–(2.9)*, equals* $\mathbf{R}^2$.

Remark 2.4. To apply Algorithm 2.1, we need to describe optimal microstructures explicitly, for which the lower Hashin–Shtrikman bound on the complementary energy is saturated. Theorem 1.1 assures that this bound is optimal and that it is saturated by a sequentially laminated microstructure. We use Theorem 5 from [13] to describe optimal microstructures, with a brief explanation where necessary.

In case (i) the optimal microstructure for which the bound is saturated is a simple laminate with layers orthogonal to $\mathbf{e}$, such that $\mathbf{e}$ is an extremal for

$$h_{\mathbf{B}}(\boldsymbol{\eta}) = \min_{\mathbf{e} \in S^1} \frac{|(\mathbf{e} \otimes \mathbf{e}) : \mathbf{B}\boldsymbol{\eta}|^2}{\mathbf{B}(\mathbf{e} \otimes \mathbf{e}) : (\mathbf{e} \otimes \mathbf{e})}, \tag{2.10}$$

where $h_{\mathbf{B}}$ is a function of the extremal $\boldsymbol{\eta}$ in (1.8). According to Lemma 4 of [14], $\mathbf{e}$ is the eigenvector associated with an eigenvalue of the least absolute value of $\boldsymbol{\eta}$.

Similarly, in case (ii) the optimal microstructure for which the bound is saturated is a simple laminate with layers orthogonal to $\mathbf{e}$, such that $\mathbf{e}$ is an extremal for (2.10). Due to results shown in [13], in this case $h_{\mathbf{B}}(\boldsymbol{\eta})$ equals zero, for $\boldsymbol{\eta}$ which is extremal in (1.8). Thus, one has to find $\mathbf{e}$ such that $(\mathbf{B}\boldsymbol{\eta})\mathbf{e} \cdot \mathbf{e} = 0$. After performing a simple calculation, the first component of this unit vector in the basis of eigenvectors of $\boldsymbol{\sigma}$ satisfies

$$\mathbf{e}_1^2 = \frac{1}{2}\left[1 - \frac{\delta\kappa(\mu_{\mathbf{B}} - \theta\delta\mu)(\sigma_1 + \sigma_2)}{\delta\mu(\kappa_{\mathbf{B}} - \theta\delta\kappa)(\sigma_1 - \sigma_2)}\right].$$

In case (iii) the optimal microstructure for which the bound is saturated is a rank-2 laminate with directions of lamination given by eigenvectors $\mathbf{v}_1$ and $\mathbf{v}_2$ of $\boldsymbol{\sigma}$, and corresponding lamination parameters

$$m_1 = \frac{2(1-\theta)\mu_{\mathsf{B}}\delta\kappa\sigma_2 - \kappa_{\mathsf{A}}(\mu_{\mathsf{B}}+\kappa_{\mathsf{B}})(\sigma_1-\sigma_2)}{2(1-\theta)\mu_{\mathsf{B}}\delta\kappa(\sigma_1+\sigma_2)},$$
$$m_2 = \frac{2(1-\theta)\mu_{\mathsf{B}}\delta\kappa\sigma_1 + \kappa_{\mathsf{A}}(\mu_{\mathsf{B}}+\kappa_{\mathsf{B}})(\sigma_1-\sigma_2)}{2(1-\theta)\mu_{\mathsf{B}}\delta\kappa(\sigma_1+\sigma_2)}.$$

Remark 2.5. From Theorem 2.3 can be deduced that a zero of the function

$$\theta \mapsto \frac{\partial h}{\partial \theta}(\theta, \boldsymbol{\sigma}(\mathbf{x})) + l$$

can be explicitly calculated from quadratic or quartic equation a.e. on Ω.

3. Numerical examples

In this section we present several examples of optimal design problems for elastic plate in two space dimensions using Algorithm 2.1. In all examples we consider compliance minimization

$$\int_\Omega f u \,\mathrm{d}\mathbf{x} \longrightarrow \min.$$

Here u is the solution of Kirchhoff–Love plate equation

$$\begin{cases} \mathsf{div}\,\mathsf{div}\,(\mathbf{M}\nabla\nabla u) = f \text{ in } \Omega \\ u \in \mathrm{H}_0^2(\Omega). \end{cases} \tag{3.1}$$

The implementation of the algorithm is made using `FreeFem++` [27]. The nonconforming quadratic Morley finite elements on a triangular mesh are used to find a solution of elastic plate equation (3.1) [10,35]. Moreover, piecewise constant elements on a triangular mesh are used to describe a design $(\theta^k, \mathbf{M}^k)$.

To determine the exact Lagrange multiplier a simple secant method is utilized. Specifically, in each iteration, we find the Lagrange multiplier that satisfies $\int_\Omega \theta^k(\mathbf{x})\,\mathrm{d}\mathbf{x} = q$. This ensures that the amount of the materials remains fixed throughout the simulation.

After obtaining the final result through the homogenization part, we introduce a simple penalization technique based on the previous results [3]. The only difference from Algorithm 2.1 is in the second step: instead of taking θ^{k+1} as the optimal proportion for the next iteration, we replace it with

$$\theta^{k+1}_{\mathrm{pen}} := \frac{1-\cos\left(\pi\theta^{k+1}\right)}{2}. \tag{3.2}$$

As such, $\theta^{k+1}_{\mathrm{pen}}$ will be closer to 0 or 1 than θ^{k+1}, since if $0 < \theta^{k+1} < \frac{1}{2}$ then $\theta^{\mathrm{pen}} < \theta^{k+1}$, while if $\frac{1}{2} < \theta^{k+1} < 1$ then $\theta^{\mathrm{pen}} > \theta^{k+1}$. For the penalization method, again we determine the precise Lagrange multiplier using the secant method. In this way, a classical design will be obtained, at the cost of a slightly greater compliance functional.

3.1. Compliance minimization on a square

For the first example we take the domain to be a clamped square plate, $\Omega = [0,1]\times[0,1]\,\mathrm{m}^2$, subjected to a uniform pressure $f = 1\,\mathrm{GPa}$. We take the stronger material with Young's modulus $E_{\mathsf{B}} = 34.5\,\mathrm{GPa}$ and Poisson's ratio $\nu_{\mathsf{B}} = 0.3$, and the weaker material with the same Poisson's ratio, while $E_{\mathsf{A}} = 0.06E_{\mathsf{B}}$. Moreover, we assume that the stiffness tensor $\mathbf{M}$ is made up of 50% of the first (weaker) material. The domain was triangulated with

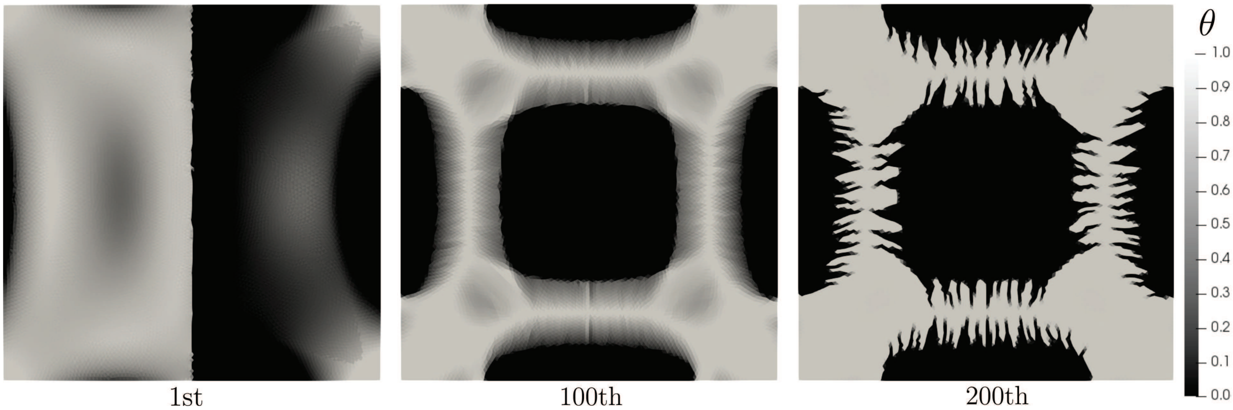

FIGURE 1. Optimal and penalized design for the problem presented in Section 3.1.

23 000 triangles, and the mesh size was set to 1.5×10^{-2} m. We prescribe the initial design $(\theta^0, \mathbf{M}^0)$ on the following way: for $\theta^0 : \Omega \to [0,1]$ we take

$$\theta^0(x,y) = \begin{cases} 1, & x < 0.75, \\ 0, & x \geq 0.75, \end{cases}$$

resulting $\mathbf{M}^0$ to be a pure material $\mathbf{B}$ on the right side of the domain, and a pure material $\mathbf{A}$ on the left one.

The optimal design of the first and 100th iteration is given in Figure 1. The black color indicates the stronger material, while the weaker material is represented by paper white. The gray tones correspond to composite materials. Since the initial design is not symmetrical, we may observe a loss of symmetry in the first few iterations.

We have found that this optimal design is quite close to one in [21], where similar problem was considered regarding shape optimization. To retrieve a classical design, additional 100 iterations of the algorithm with penalty function (3.2) were performed. We present the penalized design obtained at the 200th iteration of the algorithm in Figure 1, where composite materials were compensated with spikes in the domain.

A notable reduction in compliance functional during the initial stages of the homogenization method occured, as can be seen in Figure 2, succeeded by a modest uptick subsequent to the implementation of the penalization method. Specifically, the compliance functional experienced a mere 4.3% increase post-penalization. As a convergence criterion we use L^2 norm of the difference θ between two consecutive iterations, expressed as $\|\theta^k - \theta^{k-1}\|_{L^2}$. This criterion is visually depicted in Figure 2. It is important to note that the final optimal design does not depend on the choice of the initial design. In fact, we can even ignore the prescribed volume of materials and start with only the weaker material **A** or the stronger material **B**.

3.2. Compliance minimization on a circle – impact of the mesh refinement

Let $\Omega = B((0,0),1)$ be a ball with a radius of 1 m, where a uniform pressure $f = 10\,\mathrm{MPa}$ is present. The Young's moduli and Poisson's ratios of weaker and stronger materials are $E_{\mathbf{A}} = 3.45\,\mathrm{GPa}$, $\nu_{\mathbf{A}} = 0.3$, and $E_{\mathbf{B}} = 34.5\,\mathrm{GPa}$, $\nu_{\mathbf{B}} = 0.3$, respectively, while the amount of the first material is set to 30%. The initial design $(\theta^0, \mathbf{M}^0)$ is radial, with weaker material present in the inner part, creating a ball that occupies 75% of the domain. We conducted simulations on various triangulations of Ω. All meshes were uniformly discretized, and the respective mesh sizes and triangle counts are detailed in the accompanying Table 1, as well as values of the compliance functional at the 100th iteration of Algorithm 2.1.

A finer mesh size allows for a more accurate approximation of the state function u and its second-order derivatives, crucial components in the homogenization algorithm. Additionally, this refinement provides enhanced

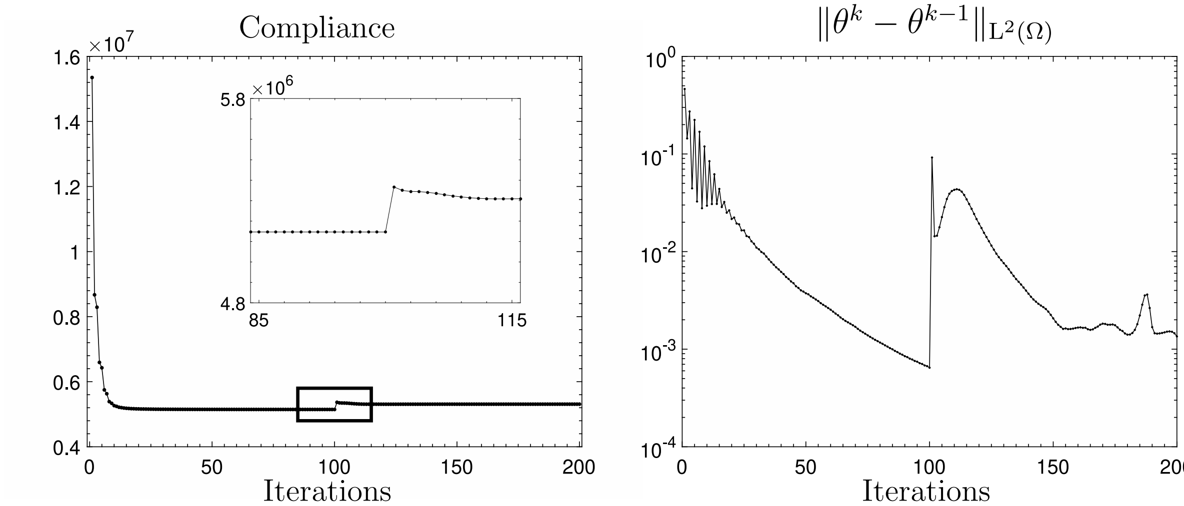

FIGURE 2. Compliance functional and L^2 norm error for θ between iterations for the problem presented in Section 3.1.

TABLE 1. The final compliance results for both the homogenization and penalization components of the algorithm in relation to the refinement of the triangulation for the problem presented in Section 3.2.

Label	1	2	3	4	5	6
Mesh size h	0.07427	0.04951	0.03713	0.02970	0.02476	0.02122
Number of triangles	2564	5769	10256	16025	23076	31409
Compliance (homog.)	46.073	45.514	45.306	45.207	45.152	45.119
Compliance (penal.)	46.829	46.086	45.822	45.657	45.567	45.499

resolution for θ and the homogenized tensor $\mathbf{M}$. However, it is worth noting that we have observed diminishing returns regarding compliance value with higher mesh refinement, as illustrated in Table 1.

The impact of the mesh refinement on optimal design after 100 iterations of the algorithm is presented in Figure 3. Again, the black color represents the stronger material, paper white weaker material, and gray tones represent composite materials. The first, weaker material creates an annulus in the domain, with composite materials on its boundary. A fine structure seems to stabilize, with no notable differences observed in optimal design for the 5th and 6th triangulation.

For the penalization part of the algorithm differences arise with each refinement of the mesh. As depicted in Figure 4, after 100 iterations of the penalization process, various end results emerge, with outcomes highly dependent on the triangulation.

The resolution of the spikes, which compensate for the previous composite materials, appears to depend on the mesh size of triangulations. In other words, with a smaller mesh size, there are more protrusions, but with a smaller width.

The convergence history for the compliance and L^2 norm error using the 6th triangulation from Table 1 is given in Figure 5. We have observed a significant decrease in compliance during the first few iterations of the homogenization method, followed by a small increase after the penalization method was applied. More precisely, the compliance functional increased for only 0.84% after penalization.

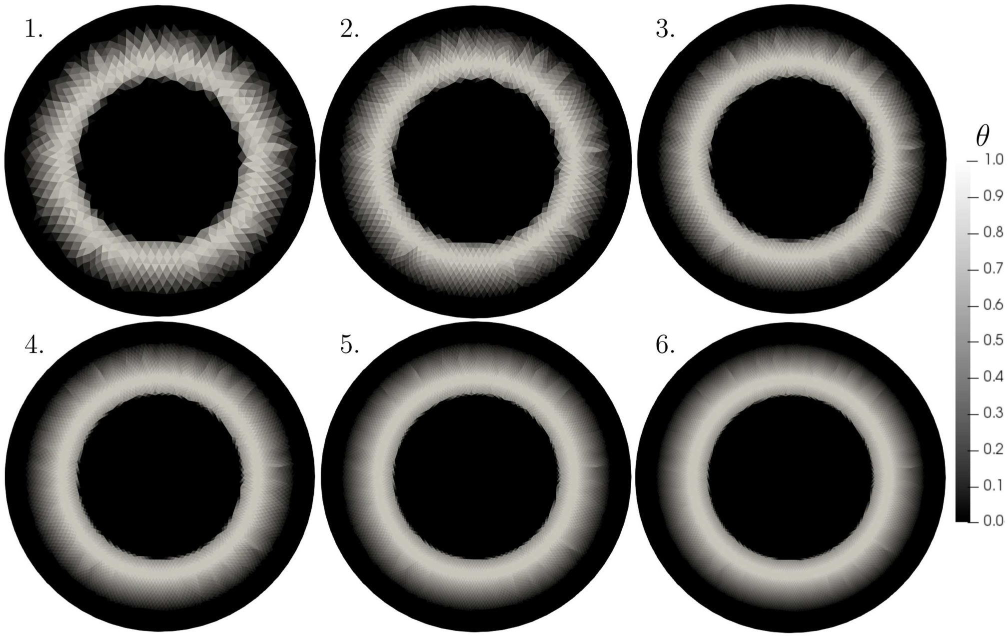

FIGURE 3. Comparison of optimal designs with different triangulations for the problem presented in Section 3.2.

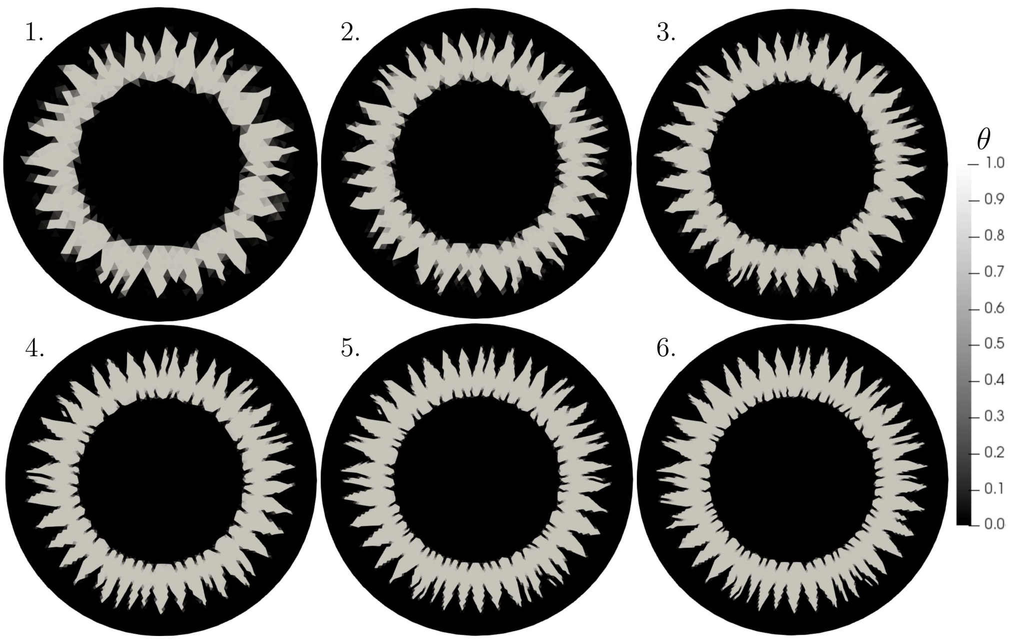

FIGURE 4. Comparison of penalized designs with different triangulations for the problem presented in Section 3.2.

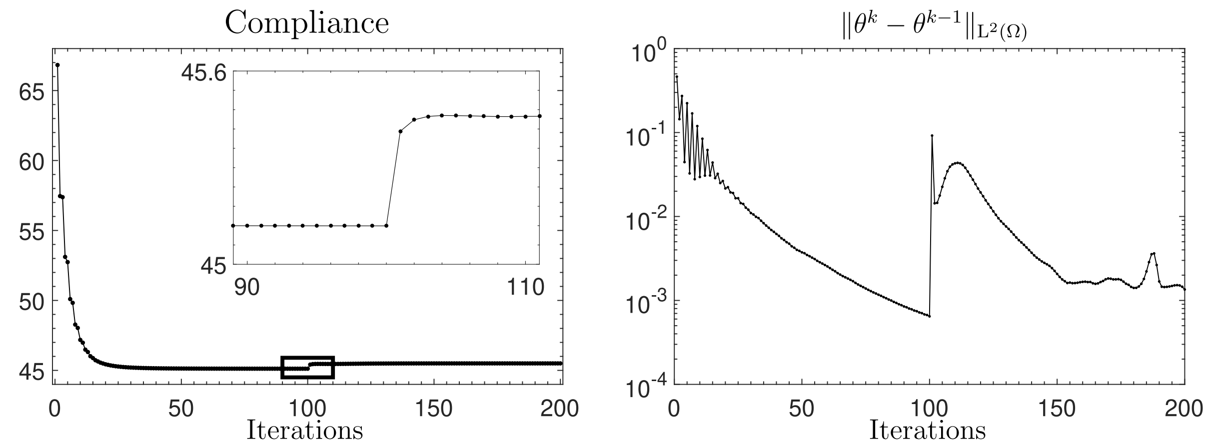

FIGURE 5. Compliance functional and L^2 norm error for θ between iterations for the problem presented in Section 3.2.

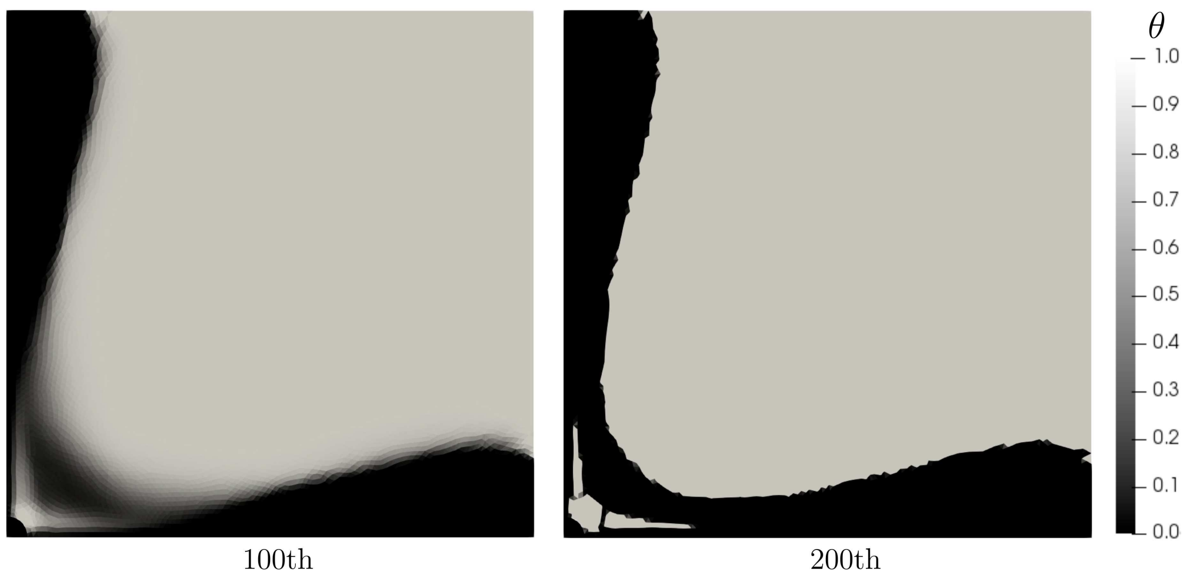

FIGURE 6. Optimal and penalized design for the problem presented in Section 3.2.

We would like to mention that executing the algorithm on various structural optimization problems in radial domains and with radial loads, and comparing results with results on similar problems in conductivity [11, 15] gives a motive for finding an explicit solution in radial case. However, due to the complexity of the elastic plate equation, and because of the fourth order derivatives, this appears to be a formidable task.

3.3. Compliance minimization with high contrast

In the last example, we consider a square plate $\Omega = [0,1] \times [0,1]\,\mathrm{m}^2$, and apply a force $f = 5\,\mathrm{kPa}$ over the area $S = \{(x,y) \in \Omega : x^2 + y^2 < 0.04^2\}$. Furthermore, in this area we set $\theta^k|_S = 0$ meaning that in S only the stronger material **B** is present.

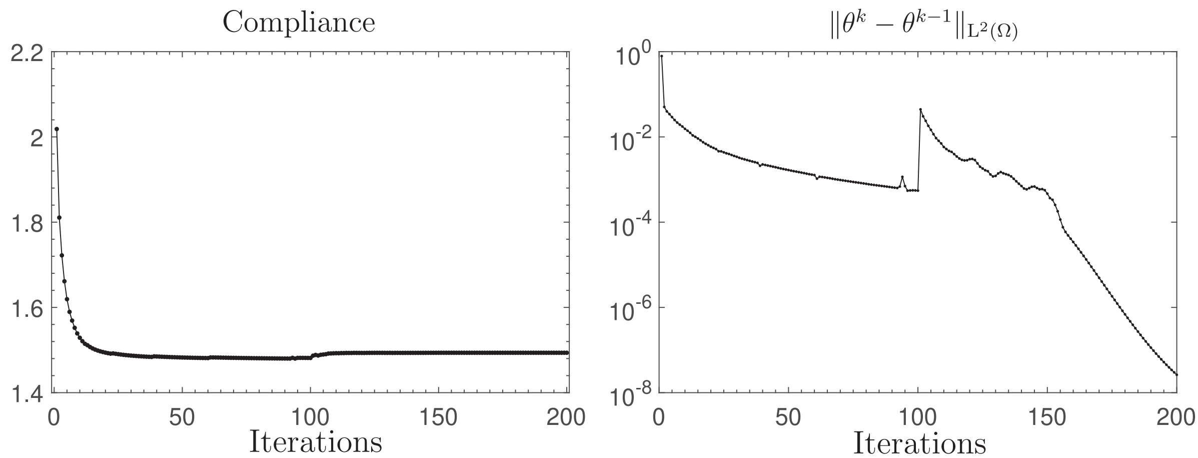

FIGURE 7. Compliance functional and L^2 norm error for θ between iterations for the problem presented in Section 3.3.

The Young's modulus of the stronger material is $E_{\mathbf{B}} = 16.87\,\text{Pa}$, and the Poisson's ratio is $\nu_{\mathbf{B}} = 0.33\,\text{Pa}$. The weaker material has the same Poisson's ratio as the stronger one, while $E_{\mathbf{A}} = 0.001E_{\mathbf{B}}$. While one could typically define $\mathbf{A}$ as even weaker, we found that such an approach increases the number of iterations needed to achieve convergence, with only slight differences in the final design. The initial design is configured with the stronger material $\mathbf{B}$, expressed as $(\theta_0, \mathbf{M}_0) = (0, \mathbf{B})$.

Numerical solutions for the optimal and penalized designs are given in Figure 6, where the 100th iteration of Algorithm 2.1 is presented for both designs. These results are very similar to those in [38] where topology optimization problem with the same assumptions was considered. This suggests that the algorithm's end result serves as an excellent initial guess for material-void optimization, with potential for further enhancement through shape or topology optimization. The convergence history for both compliance and the L^2 norm error is illustrated in Figure 7. After penalization process, the compliance functional increased for 0.36%.

Acknowledgements

The authors thank the reviewers for their useful comments that contributed to improve substantially the quality of this paper.

Funding

Ivana Crnjac and Jelena Jankov Pavlović have been supported in part by Croatian Science Foundation under projects 8904 Homdirestroptcm and 5181 HOMeoS. Petar Kunštek is partially supported by the Croatian Science Foundation under project 7261 ADESO.

References

[1] J. Aboudi, Mechanics of Composite Materials: Studies in Applied Mechanics. Elsevier, Amsterdam (1991).

[2] G. Allaire, Explicit lamination parameters for three-dimensional shape optimization. *Control Cybern.* **23** (1994) 309–326.

[3] G. Allaire, Shape optimization by the homogenization method, in Applied Mathematical Sciences. Springer (2001).

[4] G. Allaire and R.V. Kohn, Explicit optimal bounds on the elastic energy of a two-phase composite in two space dimensions. *Q. Appl. Math.* **51** (1993) 675–699.

[5] G. Allaire and R.V. Kohn, Optimal design for minimum weight and compliance in plane stress using extremal microstructures. *Eur. J. Mech. A/Solids* **12** (1993) 839–878.

[6] G. Allaire, E. Bonnetier, G. Francfort and F. Jouve, Shape optimization by the homogenization method. *Numer. Math.* **76** (1997) 27–68.

[7] N. Antonić and N. Balenović, Optimal design for plates and relaxation. *Math. Commun.* **4** (1999) 111–119.

[8] N. Antonić and N. Balenović, Homogenisation and optimal design for plates. *Z. Math. Mech.* **80** (2000) 757–758.

[9] M.P. Bendsøe, Optimization of Structural Topology, Shape, and Material. Vol. 414. Springer (1995).

[10] S.C. Brenner and L. Ridgway Scott, The Mathematical Theory of Finite Element Methods. Vol. 3. Springer (2008).

[11] K. Burazin, Unique solutions of multiple-state optimal design problems on an annulus. *J. Optim. Theory App.* **177** (2018) 329–344.

[12] K. Burazin and I. Crnjac, Application of explicit energy bounds in optimization of 3D elastic structures. *Optim. Eng.* (2023). DOI: 10.1007/s11081-023-09840-w.

[13] K. Burazin and J. Jankov, Explicit bounds on the energy and moduli of a composite elastic plate, under review.

[14] K. Burazin and J. Jankov, On the effective properties of composite elastic plate. *J. Math. Anal. App.* **495** (2021) 124696.

[15] K. Burazin and M. Vrdoljak, Exact solutions in optimal design problems for stationary diffusion equation. *Acta Appl. Math.* **161** (2019) 71 –88.

[16] K. Burazin, J. Jankov and M. Vrdoljak, Homogenization of elastic plate equation. *Math. Modell. Anal.* **23** (2018) 190–204.

[17] K. Burazin, I. Crnjac and M. Vrdoljak, Optimality criteria method in 2D linearized elasticity problems. *Appl. Numer. Math.* **160** (2021) 192–204.

[18] K. Burazin, I. Crnjac and M. Vrdoljak, Explicit Hashin-Shtrikman bounds in 3D linearized elasticity, under review.

[19] J. Casado-Díaz, C. Castro, M. Luna-Laynez and E. Zuazua, Numerical approximation of a one-dimensional elliptic optimal design problem. *Multiscale Model. Simul.* **9** (2011) 1181–1216.

[20] R. Christensen, Mechanics of Composite Materials. John Wiley, New York (1979).

[21] G. Dzierżanowski, Stress energy minimization as a tool in the material layout design of shallow shells. *Int. J. Solids Struct.* **49** (2012) 1343–1354.

[22] G.A. Francfort and F. Murat, Homogenization and optimal bounds in linear elasticity. *Arch. Ration. Mech. Anal.* **94** (1986) 307–334.

[23] L.V. Gibiansky and A.V. Cherkaev, Design of composite plates of extremal rigidity. Ioffe Physicotechnical Institute preprint (1984).

[24] L.V. Gibiansky and A.V. Cherkaev, Microstructures of composites of extremal rigidity and exact bounds of the associated energy density. Ioffe Physicotechnical Institute preprint (1987).

[25] L.V. Gibiansky and A.V. Cherkaev, Design of composite plates of extremal rigidity, in Topics in the Mathematical Modelling of Composite Materials. Modern Birkhäuser Classics. Birkhäuser (2018) 95–137.

[26] Z. Hashin and Z. Shtrikman, A variational approach to the theory of the elastic behaviour of multiphase materials. *J. Mech. Phys. Solids* **11** (1963) 127–140.

[27] F. Hecht, New development in FreeFem++. *J. Numer. Math.* **20** (2012) 251–266.

[28] V.V. Jikov, S.M. Kozlov and O.A. Oleinik, Homogenization of Differential Operators and Integral Functionals. Springer Science & Business Media (2012).

[29] R. Kohn and G. Strang, Optimal design and relaxation of variational problems I–III. *Commun. Pure Appl. Math.* **39** (1986) 113–137, 139–182, 353–377.

[30] K.A. Lurie and A.V. Cherkaev, Exact estimates of conductivity of composites formed by two isotropically conducting media taken in prescribed proportion. *Proc. R. Soc. Edinburgh Sect. A: Math.* **99** (1984) 71–87.

[31] K.A. Lurie and A.V. Cherkaev, Effective characteristics of composite materials and the optimal design of structural elements. *Uspekhi Mekhaniki* **9** (1986) 3–81.

[32] K.A. Lurie, A.V. Cherkaev and A.V. Fedorov, Regularization of optimal design problems for bars and plates I–II. *J. Optim. Theory App.* **37** (1982) 499–522.

[33] G. Milton, The Theory of Composites. Cambridge University Press (2001).

[34] G. Milton, M. Briane and D. Harutyunyan, On the possible effective elasticity tensors of 2-dimensional and 3-dimensional printed materials. *Math. Mech. Complex Syst.* **5** (2017) 41–94.

[35] L.S.D. Morley, The triangular equilibrium element in the solution of plate bending problems. *Aeron. Q.* **19** (1968) 149–169.

[36] F. Murat and L. Tartar, H-convergence, in séminaire d'analyse fonctionnelle et numérique de l'université d'alger. Lecture Notes (1978).

[37] F. Murat and L. Tartar, Calcul des variations et homogénéisation, in: Les méthodes de l'homogenisation théorie et applications en physique, bréausans-nappe. **57** (1985) 319–369.

[38] A.A. Novotny, R.A. Feijóo, C. Padra and E. Taroco, Topological derivative for linear elastic plate bending problems. *Control Cybern.* **34** (2005) 339–361.

[39] G.I. Rozvany, Structural Design and Optimality Criteria. Kluwer Academic Publisers (1989).

[40] L. Tartar, Remarks on homogenization, in Homogenization and Effective Moduli of Materials and Media. Springer (1986) 228–246.

[41] L. Tartar, The General Theory of Homogenization: A Personalized Introduction. Vol. 7. Springer Science & Business Media (2009).

[42] M. Vrdoljak, Classical optimal design in two-phase conductivity problems. *SIAM J. Control Optim.* **54** (2016) 2020–2035.